

Phase-shifted Bragg grating-based Mach-Zehnder Interferometer Sensor using an Intensity Interrogation Scheme

Enxiao Luan^{1,*}, Han Yun^{1,*}, Stephen H. Lin¹, Karen C. Cheung¹, Lukas Chrostowski¹ and Nicolas A. F. Jaeger¹

¹*Department of Electrical and Computer Engineering, The University of British Columbia, 2332 Main Mall, Vancouver, BC, V6T 1Z4, Canada*

**These authors contributed equally to this work.*

eluan@ece.ubc.ca

Abstract: We experimentally demonstrated the suitability of the phase-shifted Mach-Zehnder interferometric device to support real-time sensing monitoring using an intensity interrogation scheme. The proposed sensor presents a sensitivity of ~ 810 dB/RIU with a broadband light source. © 2020 The Author(s)

OCIS codes: 000.0000, 999.9999.

1. Introduction

Optical biosensors have had and will continue to have a huge impact on analytical technology for the detection of biological and chemical targets [1]. Plenty of optical biosensors have found applications in healthcare, environmental monitoring, clinical diagnostics, and biotechnology industry in the past decades. Among them, evanescent field detection is the major detection principle of most optical sensors. Due to the high optical waveguide confinement and mature CMOS-compatible foundries, silicon photonic evanescent field-based sensors enable high-sensitivity analysis with a miniaturized size, as well as low-cost, large-scale manufacturing. Moreover, existing CMOS fabs allow one to integrate the light source, the sensor device, and the photodetector (PD) onto a single silicon die, which gives the potential to build complete lab-on-a-chip sensing systems.

A large variety of optical architectures have emerged leveraging the silicon substrate for sensing applications. Based on different architectures, different signal interrogation schemes are employed. However, most approaches demand either a wavelength-tunable light source or a high-resolution readout system for precise optical spectrum scanning and processing, which increases the overall cost of the sensing system. Intensity interrogation schemes have been demonstrated as an alternative solution for sensing, due to their capability for operating the system with a low-cost broadband source input and a relative intensity measurement as the output [2]. Several relevant architectures have been published to reduce the system cost by using a broadband light source, such as a light-emitting diode (LED) or a superluminescence diode (SLD) [3,4].

In this work, we present a Mach-Zehnder interferometer-based sensing architecture with a cost-effective intensity interrogation scheme, in which both symmetric arms (sensing and reference arms) consist of a phase-shifted Bragg grating (PSBG). Although similar architectures have been reported by combining resonators and an MZI structure for high-performance modulation [5,6], to our knowledge, this is the first experimental demonstration of sensing using an intensity interrogation method. As shown in Fig. 1(a), when we introduce a solution containing target molecules into the sensing arm, due to the refractive index (RI) change, the phase at the resonant peak changes at the output, and the destructive interference occurs when combined with the light from the reference arm. Thus, an intensity interrogation method can be applied to detect the RI change in real-time.

2. Design and Modelling

Bragg grating waveguides have been widely applied for telecommunications as part of filters, modulators or semiconductor lasers. When a phase-shifted configuration is added in the center, gratings on each side can be treated as pseudo-mirrors, which form a first-order Fabry-Perot (FP) resonant cavity and generates a single resonant peak in the middle of the stopband. By tracking the peak wavelength shift, phase-shifted Bragg grating-based resonators can be employed for use in biosensing. In the case of the phase-shifted cavity of a length of $\Lambda/2$ (as shown in the dashed box in Fig. 1(b)), the phase-shifted section will give a π phase shift at the center wavelength of the stopband, where Λ is the period of the grating. In a conventional Mach-Zehnder interferometer, the intensity at the output is periodically oscillated based on the phase difference of two arms. In terms of sensing, the sensitivity

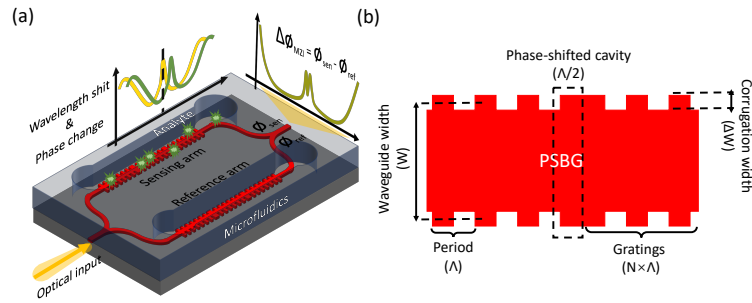


Fig. 1: (a) Schematic of the Bragg grating-based Mach-Zehnder interferometer (PSBG-MZI) sensing architecture, showing a phase change (ϕ_{sen}) at the output of the sensing arm due to the analyte attachment. (b) Schematic of the PSBG in both arms, and the phase-shifted cavity in the middle. W is the waveguide width, ΔW is the corrugation width, Λ is the period, and N is the number of periods of the grating on each side.

of an MZI sensor is usually related to the length of the sensing arm, typically on the order of the millimeter. The combination of Bragg grating resonators and MZIs can increase the analyte interaction while maintaining a small footprint. Grating parameters of the PSBG were optimized by using Bloch boundary conditions on one grating periodic cell through a fully vectorized three-dimensional Finite-Difference-Time-Domain (3D-FDTD) approach for band structure calculations. By adjusting the period ($\Lambda = 315$ nm) and corrugation width ($\Delta W = 70$ nm) of the grating cell, the central wavelength of the stopband appears near 1550 nm in the TE mode.

3. Results and Discussions

Our proposed PSBG-MZI devices were designed through KLayout with the Process Design Kit (SiEPIC-EBeam-PDK) [7], and fabricated on silicon-on-insulator (SOI) chips by the direct-write 100 keV electron-beam lithography (EBL, JEOL JBX-810OFS). As SEM images presented in Fig. 2, the PSBG-MZI architecture consists of two symmetric PSBG-based waveguides, where each PSBG has a phase-shifted cavity at the center (Fig. 2(b)). Two Y-branches are used to split and recombine the guided light through the MZI architecture, with an insertion loss of approximately 3.3 dB (Fig. 2(c)).

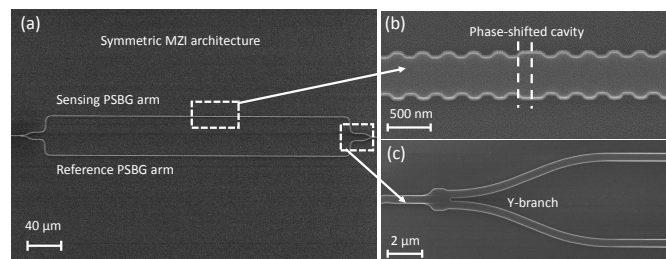


Fig. 2: (a) SEM image of the PSBG-MZI architecture, which includes one sensing arm and one reference arm. (b) Amplified SEM image of the PSBG structure in the phase-shifted cavity. (c) Amplified SEM image of the Y-branch used in the cascaded PSBG-MZI.

For the intensity interrogation, we used a cost-effective broadband LED (BeST-SLED) as the optical input. The broadband source was then passed through a tunable optical super-Gaussian filter (OTF-950) with the bandwidth of 3 nm and an erbium-doped fiber amplifier (EDFA-C-26G-S) to filter out unnecessary wavelengths and compensate for the losses. After passing through the sensing device, the total intensity of the light was detected by the power detector (Agilent 81653A). The schematic of the PSBG-MZI sensing system is shown in Fig. 3 below. A temperature controller (LDC501) was used to control the platform temperature. All sensing architectures were aligned underneath a poly(dimethylsiloxane) (PDMS) microfluidics. A syringe pump (Chemyx Nexus 3000) was employed to control flow rates by withdrawing reagents over the sensors.

Sensor performance was characterized by using a series of IPA solutions and layer-by-layer electrostatic polymer depositions. After calibrating out the insertion losses from the system (including the losses from grating couplers, routing waveguides, fiber connections, etc.), measured sensing results are depicted in Fig. 4. By injecting IPA dilutions from 1% to 10% (v/v) to the sensing arm sequentially, while keeping ID water flow in the reference arm, the total power intensity detected at the output was measured as a function of time, showing an averaged bulk sensitivity of about 810 dB/RIU (Fig. 4(a)). The temperature was controlled at 25°C during the experiment to eliminate the thermal noise. However, due to the sinusoidal shape of the interferometric spectrum, the phase variation-caused intensity change versus the RI change is not a linear function, which is one of the main draw-

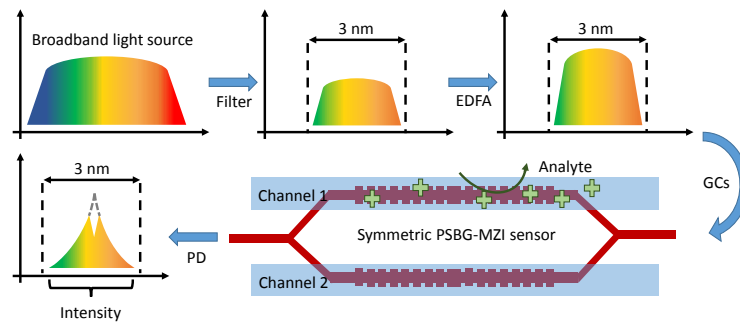


Fig. 3: Schematic of the proposed PSBG-MZI sensing system for the intensity interrogation.

backs of MZI-based sensors. Therefore, to evaluate the non-linear sensor response, we introduced a layer-by-layer electrostatic polymer deposition approach (similar to Ref. [8]) by continuously injecting polystyrene sulfonate (PSS) and polyallylamine hydrochloride (PAH) to the sensor. After the initial adhesion of positively charged PEI to ensure sufficient coverage, PSS/PAH bilayers were deposited on the sensing arm surface. Each deposition was followed with a 5-min Tris buffer flushing to avoid precipitation and clogging. The sensorgram is depicted in Fig. 4(b), showing a sinusoidal intensity variation at the output. If we assume the thickness of the bilayer is constant (1.99 nm), the highest intensity change happens at $\pi/2$ phase difference of two arms, approximately 0.76 dB/nm. Therefore, to obtain the best sensor performance of the proposed PSBG-MZI sensor, an initial $\pi/2$ phase difference is needed, which can be realized by using a heater or injecting a high RI solution to one of the arms.

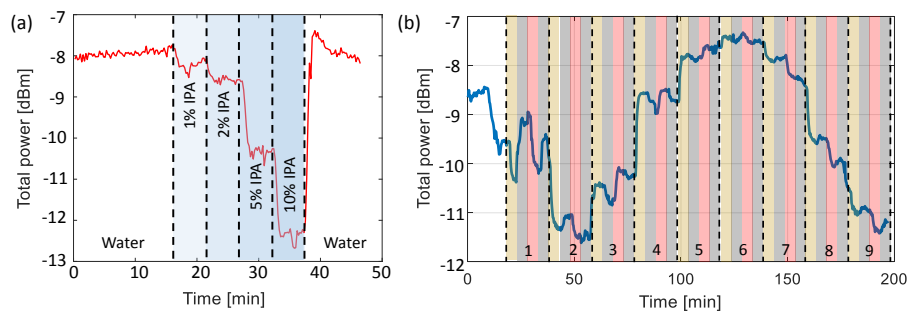


Fig. 4: (a) Calibrated power intensity at the output of the proposed PSBG-MZI sensor with various concentrations of IPA injected as a function of time. (b) Calibrated power intensity in terms of the deposition of polymers at the sensor surface. Yellow and pink areas represent the PSS and PAH injection. Grey areas are the Tris buffer rinse.

References

1. L. M. Lechuga, "Optical biosensors," *Comprehensive analytical chemistry* **44**, pp. 209–250, 2005.
2. P. R. Prasad, S. K. Selvaraja, and M. M. Varma, "Full-range detection in cascaded microring sensors using thermo-optical tuning," *Journal of Lightwave Technology* **34**(22), pp. 5157–5163, 2016.
3. J. Song, X. Luo, X. Tu, M. K. Park, J. S. Kee, H. Zhang, M. Yu, G.-Q. Lo, and D.-L. Kwong, "Electrical tracing-assisted dual-microring label-free optical bio/chemical sensors," *Optics express* **20**(4), pp. 4189–4197, 2012.
4. L. Dias, E. Luan, H. Shoman, H. Jayatileka, S. Shekhar, L. Chrostowski, and N. A. F. Jaeger, "Cost-effective, cmos-compatible, label-free biosensors using doped silicon detectors and a broadband source," in *CLEO: Applications and Technology*, pp. ATu4K–5, Optical Society of America, 2019.
5. Y. Terada, K. Kondo, R. Abe, and T. Baba, "Full c-band si photonic crystal waveguide modulator," *Optics letters* **42**(24), pp. 5110–5112, 2017.
6. O. Jafari, H. Sephrian, W. Shi, and S. LaRochelle, "High-efficiency silicon photonic modulator using coupled bragg grating resonators," *Journal of Lightwave Technology* **37**(9), pp. 2065–2075, 2019.
7. L. Chrostowski, H. Shoman, M. Hammood, H. Yun, J. Jhoja, E. Luan, S. Lin, A. Mistry, D. Witt, N. A. F. Jaeger, *et al.*, "Silicon photonic circuit design using rapid prototyping foundry process design kits," *IEEE Journal of Selected Topics in Quantum Electronics*, 2019.
8. E. Luan, H. Yun, M. Ma, D. M. Ratner, K. C. Cheung, and L. Chrostowski, "Label-free biosensing with a multi-box sub-wavelength phase-shifted bragg grating waveguide," *Biomedical optics express* **10**(9), pp. 4825–4838, 2019.